

Re-examining the thermal mixing layer with numerical simulations

S. M. de Bruyn Kops^{a)} and J. J. Riley

Department of Mechanical Engineering, University of Washington, Box 352600, Seattle, Washington 98195-2600

(Received 14 July 1999; accepted 20 September 1999)

The question of whether a temperature mixing layer evolves in a self-similar manner is of importance in developing and validating theories about scalar mixing. The simplicity of the flow encourages the thought that it is self-similar, but several laboratory experiments at moderate Peclet numbers have found inconsistencies with self-similar behavior. The experimentalists are limited, however, by the length of the wind tunnels and by difficulties in aligning the virtual origins of the scalar and velocity fields. Direct numerical simulations virtually eliminate both these problems, and large-eddy simulations add the ability to study an approximation to the case of an infinite Peclet number. These two simulation techniques are used in this paper to show that the mixing layer at a moderate Peclet number very nearly evolves with a single length and time scale, and that behavior consistent with self-similarity is observed in the case of an infinite Peclet number. In addition, the results show that direct numerical simulations can accurately reproduce the data from wind tunnel experiments downstream of a turbulence grid, and that large-eddy simulations are a valuable research tool for studying the large-scale characteristics of mixing. © 2000 American Institute of Physics. [S1070-6631(00)00801-1]

I. INTRODUCTION

A thermal mixing layer is a fundamental flow in which transport of an inhomogeneous passive scalar occurs in decaying, homogeneous, isotropic turbulence. It is initiated by establishing a step change in temperature in the direction perpendicular to a steady flow downstream of a grid; the configuration is shown schematically in Fig. 1, and the coordinate system and various quantities are defined there for reference. The flow is of interest because, while being relatively easy to study, it involves physical phenomena, such as mean advection and molecular mixing, which must be accounted for in theories of scalar transport. Scalar mixing layers can also involve diffusive interfaces between reacting species, rather than changes in temperature; such flows are valuable for studying nonpremixed turbulent combustion.^{1,2} For these reasons the mixing layer has been the focus of significant experimental study beginning with Watt and Baines,³ who showed that the spread of the scalar is approximately described by a constant turbulent diffusivity. Using the data of Foss *et al.*⁴ to support theoretical arguments, Libby⁵ reached the same conclusion, and found excellent agreement for the distribution of the mean scalar in terms of a similarity variable. Throughout the early 1980's, researchers wrestled with the apparent paradox that the experimentally measured mean and rms scalar distributions (and some higher order moments) very nearly collapse when plotted against a similarity variable, but the magnitude of the heat flux is not consistent with a self-preserving flow.⁶⁻⁹ Independent experiments were conducted by different research groups on thermal mixing layers in which the initial tempera-

ture profile was introduced either upstream of the turbulence generating grid via a toaster in the inlet plenum, or at the grid by heating portions of the mesh, or downstream of the grid by means of a mandoline in the flow. The results were independent of the method used to introduce the scalar, and the consensus developed that the flow is not consistent with self-preservation.

The self-similarity debate has not been settled, however, because (1) the virtual origin of the scalar and velocity fields could not be made to coincide in the laboratory, which complicates the determination of the growth rate of the thermal length scale, (2) the number of integral time scales over which a fully developed mixing layer can be measured is small, and, (3) a self-similar solution is only expected in the limit of an infinite Peclet number, which may not be approachable in turbulence downstream of a grid in a wind tunnel. In numerical simulations, all three of these problems can be significantly ameliorated, if not eliminated. With the advent of massively parallel computers, accurate simulations of grid turbulence have been performed¹⁰ over significant downstream distances, and the virtual origins of the velocity and scalar fields can be made to very nearly coincide, as will be reported in this paper. Large-eddy simulations can be used to compute approximations to flows at very high Reynolds numbers, and are well suited for examining self-similarity because the large-scale statistics of interest are insensitive to the exact form of the subgrid-scale flux models.¹¹ In this paper, both direct and large-eddy simulation results are examined, and it is concluded that thermal mixing layers at wind tunnel Peclet numbers are not quite self-preserving, but that characteristics of self-similarity are observed when the Peclet number approaches infinity.

^{a)}Telephone: (206) 543-7837; fax: (206) 685-8047; electronic mail: debk@u.washington.edu

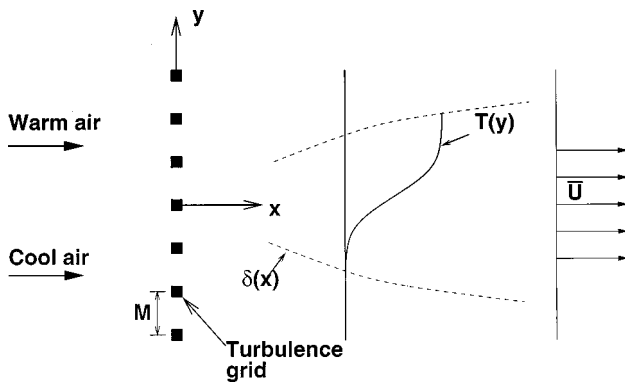


FIG. 1. Schematic of a thermal mixing layer.

II. LABORATORY EXPERIMENTS

Many of the researchers cited in the Introduction present results of earlier works in addition to their own, and discuss differences in the various sets of data. From these discussions, it is apparent that the experiments of LaRue and Libby,⁶ LaRue *et al.*,⁷ and Ma and Warhaft⁸ are the most refined, and are in close agreement with each other. Of these, the experiment of Ma and Warhaft is at a Reynolds number most suitable for direct numerical simulation on the available computers, and, for this reason only, it will form the basis of much of the discussion that follows. Various properties of the laboratory data are given in Table I.

III. DIRECT NUMERICAL SIMULATIONS

Two difficulties posed to experimentalists by the scalar mixing layer problem are those of making the virtual origins of the scalar and velocity fields coincide and of measuring data far enough downstream so that the flow is free from the effects of developing turbulence. In particular, the ratio of the thermal and mechanical length scales, δ/l , in the wind tunnel experiments is not quite constant,⁸ which introduces error when the data is examined for self-preservation. Here, δ is defined as the length from the center of the mixing layer to the point where the mean temperature is 0.92 of temperature difference across the layer, and l is the longitudinal integral length scale of the velocity field. Direct numerical simulations of decaying, homogeneous, isotropic turbulence can be accurate at moderate Reynolds numbers,¹⁰ and virtually eliminate both problems confronting the laboratory experimentalists. The direct numerical simulation method used in this research is the same as that used by de Bruyn Kops and Riley¹⁰ to accurately simulate the decaying isotropic turbulence experiment of Comte-Bellot and Corrsin.¹² Briefly, a massively-parallel, pseudo-spectral code advances the momentum and scalar transport equations in time, with all the large and small scales fully resolved. The simulations are run in a computational domain with $512 \times 512 \times 1024$ grid points. The corresponding physical size of the domain is $25.1 \times 25.1 \times 50.3$ cm. The domain is large enough that the kinetic energy transfer rate from the smallest nonzero wavenumber is small throughout the simulation, so that the periodic boundary conditions employed have negligible influence on the development of the scalar field; the maxi-

TABLE I. Properties of the laboratory experiments.

	LaRue <i>et al.</i> (1981)	Ma and Warhaft (1986) $x/M = 100$
U (cm/s)	780	620
u/U		0.014
v/U		0.012
ϵ (cm^2/s^3)		361
M (cm)	4	2.50
l (cm)		1.66
λ (cm)		0.620
η (cm)		0.0549
$\text{Re}_M = UM/\nu$	21010	9394
$\text{Re}_l = u_{\text{rms}}l/\nu$		84.8
$\text{Re}_\lambda = u_{\text{rms}}\lambda/\nu$		32.7
Test section x/M	21–67	62.4–132.4

imum resolved wavenumber times the Kolmogorov length scale ranges from 1.4 to 5.7. Taylor's hypothesis is invoked to relate the simulation time to the wind tunnel downstream distance, so that the numerical and laboratory experiments can be directly compared; temporal averaging in the laboratory corresponds to spatial averaging in the simulations. In this work, the simulations are designed to closely resemble the laboratory experiments of Ma and Warhaft,⁸ but, unlike Comte-Bellot and Corrsin, Ma and Warhaft do not provide energy spectra, and so the simulations cannot be exactly matched to the laboratory data. Velocity field data, in addition to those presented in Ma and Warhaft,⁸ are given by Sirivat and Warhaft.¹³

The scheme of de Bruyn Kops and Riley¹⁰ was used to initialize the flow field. The process yields a velocity field with well-developed turbulent structures, and with a desired kinetic energy spectrum. In the current research, only the length scales of the laboratory data are known, not the entire spectrum. Therefore, an equation for the three-dimensional kinetic energy spectrum, $E(k)$, is assumed, which approximately matches the spectrum of Comte-Bellot and Corrsin.¹² This spectrum, obtained by combining the theoretical form for the low-wavenumber production range derived by Tennekes and Lumley,¹⁴ the well-known $k^{-5/3}$ spectrum in the inertial range, and the form for the high-wavenumber dissipation range first derived by Corrsin,¹⁵ is

$$E(k) = A \exp(Bk^{-4/3})k^{-5/3} \exp(Ck^{4/3}). \quad (1)$$

The coefficients were adjusted in order to match the estimated laboratory rms velocity (u_{rms}) and integral length (l) at $x/M = 20$ (Ma and Warhaft report exact values for these parameters only at $x/M = 100$), where M is the spacing of the turbulence generating grid. The simulation was advanced to $x/M = 200$ and the decay laws $l \propto [(x-x_0)/M]^m$ and $u_{\text{rms}} \propto [(x-x_0)/M]^{m-1}$ were fitted to the resulting data. Next, the DNS spectrum at $x/M = 200$ was rescaled to approximate the spectrum at $x/M = 20$, and the simulation run again. This process was repeated, with small adjustments to the initial spectrum and Reynolds number, until convergence was obtained and the laboratory value for m was matched, to the extent practical. It is interesting to note that x_0 computed

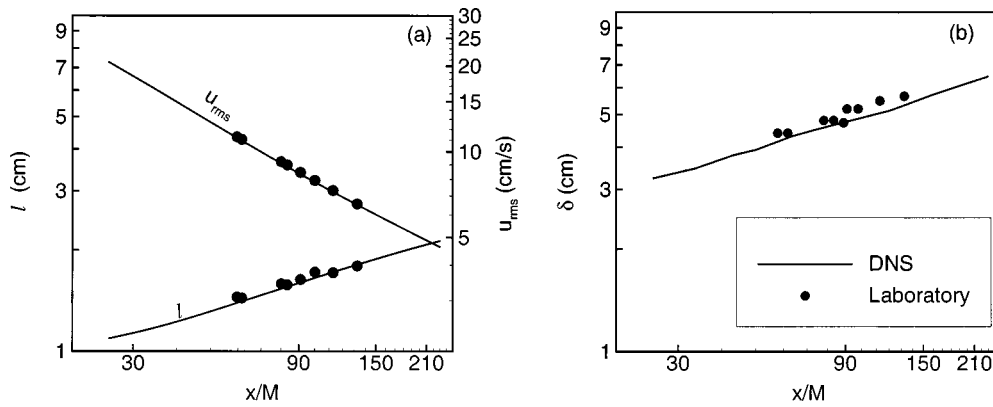


FIG. 2. Properties of the velocity and scalar fields. The symbols indicate laboratory data and the lines simulation results.

from u_{rms} differed from that computed from l by a significant amount during the first few iterations of initializing the field and advancing the simulation, but a single value of x_0 was suitable for both decay laws by the final iteration. The gross properties of the velocity field are compared with the laboratory data in Fig. 2(a).

The temperature field was initialized with an error function and allowed to evolve with the velocity field from $x/M = 25.4$ to $x/M = 33.5$. The resulting scalar field was reintroduced into the velocity field at $x/M = 25.4$, the simulation advanced to $x/M = 33.5$, and the process repeated until the width of the mean field equaled that estimated for the laboratory experiment, and the virtual origin of the scalar field coincided with that of the velocity field. The resulting scalar field has the desired large-scale properties and is roughly synchronized with the velocity field. The intent is to have a physically reasonable scalar field at $x/M = 62.4$, the location of the first laboratory data. The widths of the simulation and laboratory scalar fields are compared in Fig. 2(b).

The laboratory data⁶⁻⁸ indicate that the mean temperature profiles should approximately be error functions and

should collapse to a single profile when scaled by δ , at least to within the limit of experimental accuracy. The DNS profiles also collapse to a single error function-like form as shown in Fig. 3. The collapse over the full range from $x/M = 25.4$ to $x/M = 231$ encourages the thought that the flow is self-similar.

In Fig. 4 the mean temperature intensity profile, $I = \sqrt{\overline{\theta^2}}$, for the DNS is shown, where θ is the temperature fluctuation and the overbar denotes a spatial average. For each downstream location, the profile is normalized by I_{max} , the peak intensity at that value of x/M . As with the mean temperature, collapse to a single profile is very good in the range $-1 < y/\delta < 1$. Superimposed on the plot are the approximate mean and range (solid line and error bars) of the data from three laboratory experiments.⁶⁻⁸ The deviation from perfect collapse exhibited by the laboratory data is somewhat greater than that of the DNS data.

The maximum intensity, I_{max} , versus downstream distance is shown in Fig. 5. In their paper, Ma and Warhaft show the effect on I_{max} of a mismatch between the virtual origins of the temperature and velocity fields, and the DNS results exhibit the same behavior at low values of x/M . The fact that the DNS temperature field is not completely ad-

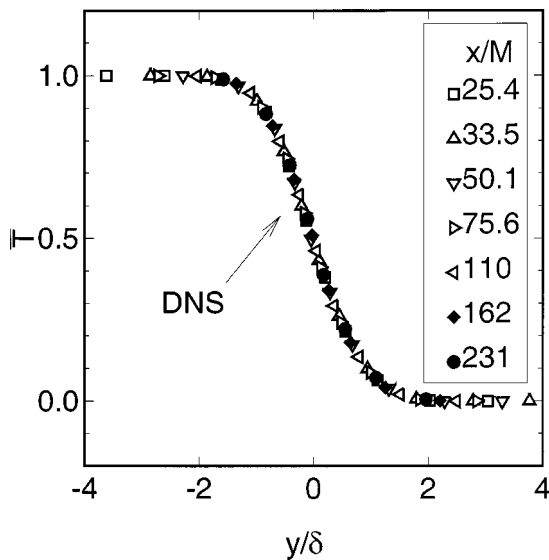


FIG. 3. Mean thermal mixing layer profiles from DNS.

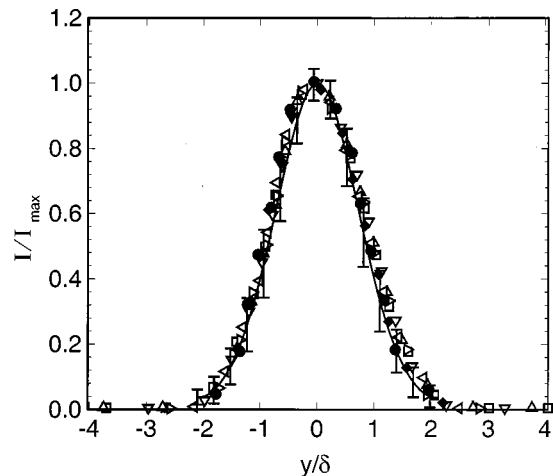


FIG. 4. Temperature fluctuation intensity profiles normalized by their peak values. Symbols are the same as for Fig. 3. The line and the error bars show the approximate mean and range of the laboratory data (Refs. 6-8).

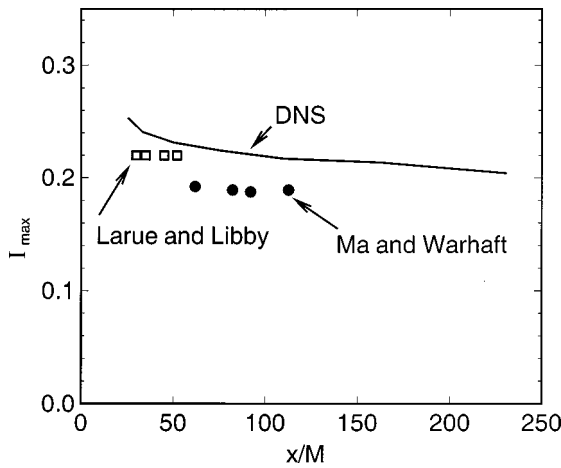


FIG. 5. Peak temperature fluctuation intensity.

justed to the velocity field at the start of the simulation, due to the method used to initialize the simulation, and evidenced by the heat flux profiles discussed below, may also explain the rapid decrease in I_{\max} in the near field. Downstream of about $x/M=50$, I_{\max} decays gently from 0.23 to 0.20, which is greater than the 0.19 reported by Ma and Warhaft, but generally less than the approximately 0.22 reported by LaRue *et al.*⁷

In Figs. 6 and 7, the DNS and laboratory measurements of the temperature skewness and kurtosis are presented, where the skewness is defined as $Sk = \overline{\theta^3}/I^3$ and the kurtosis as $Ku = \overline{\theta^4}/I^4$. In the range $-1 < y/\delta < 1$, the agreement between the laboratory and DNS results is excellent; however, the DNS results have much higher peak values for both quantities than is observed in the laboratory. The DNS results could be in error, but the most common cause of DNS inaccuracy is insufficient small-scale resolution; this would probably cause low, rather than high, predictions for these moments of the temperature fluctuations, since the temperature fluctuations would tend to be damped by the numerical solution process. Furthermore, poor resolution would likely affect high order statistics of the velocity field, such as the

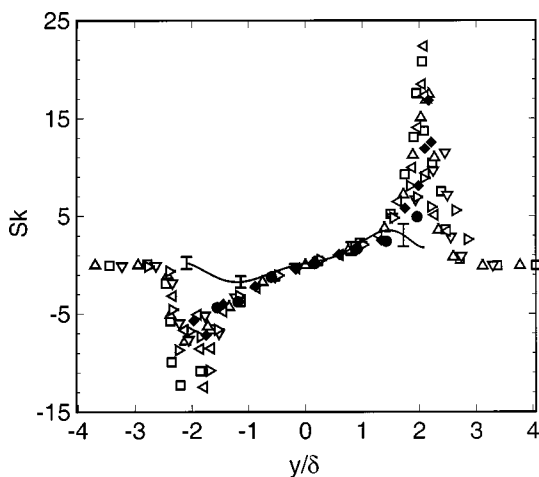


FIG. 6. Temperature skewness profiles. Symbols, line, and error bars are the same as for Fig. 4.

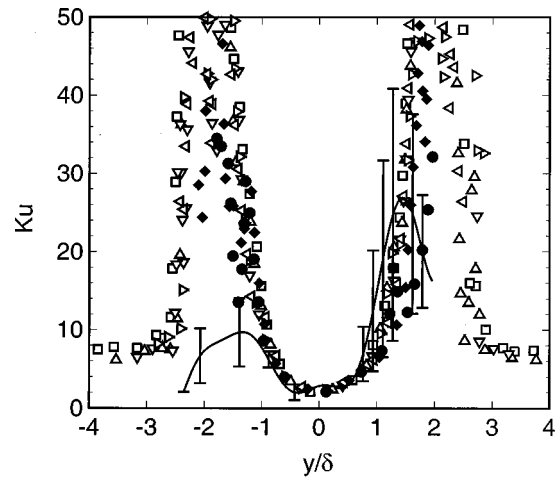


FIG. 7. Temperature kurtosis profiles. Symbols, lines, and error bars are the same as for Fig. 4.

velocity derivative skewness and flatness, but values for these quantities in the current simulations are consistent with those observed in numerous laboratory experiments.^{16,17} If the DNS results were in error due to the initial conditions, they should improve with downstream distance, but this is not the case. Another explanation for the discrepancy between the laboratory skewness/kurtosis and the DNS results is that the precision to which the temperature fluctuations can be measured in the laboratory is much lower than it is in the DNS. Ma and Warhaft report the rms noise in the instrumentation for measuring temperature to be 1/600 of the temperature difference across the layer, and only about 1/40 of I at $y/\delta = \pm 1$. In contrast, the numerical precision of the DNS calculations is about 15 orders of magnitude smaller than ΔT . It is especially noticeable in Fig. 7 that the scatter of the laboratory data is much greater on the right (low temperature) side of the plot, whereas the DNS data is approximately symmetric. This discussion suggests that the DNS data in Figs. 6 and 7 are more likely correct, and that the laboratory

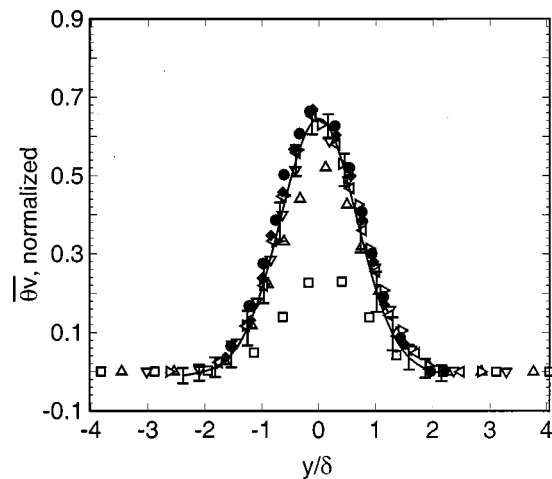


FIG. 8. Thermal flux profiles normalized by $I_{\max} \sqrt{v^2}$. Symbols, lines, and error bars are the same as for Fig. 4.

data are inaccurate where the temperature levels are very low.

Finally, the normalized heat flux profiles, $\overline{\theta v}/(I_{\max} \overline{v^2}^{1/2})$, from the DNS are shown in Fig. 8 to very closely match the laboratory profiles for $x/M > 50$. Here, v is the fluctuation of the transverse component of the velocity. In the near field, the correlation between the temperature and velocity fields is low, but increases rapidly with downstream distance, consistent with the rapid drop in I_{\max} displayed in Fig. 4.

IV. SIMILARITY SOLUTION

Given the relative simplicity of the thermal mixing layer, it is not unreasonable to expect the flow to develop in a self-similar manner, and demonstrating that the flow is self-similar has important implications in turbulence modeling. In fact, a commonly used model for closing the Reynolds averaged Navier Stokes equations for the flow^{18,19} does allow a self-similar solution. Several researchers have explored the issue in depth⁵⁻⁹ with Ma and Warhaft⁸ and Lumley⁹ finally concluding that, while profiles of the mean scalar, scalar variance, and some higher moments of the scalar intensity collapse when plotted in similarity form, the mixing layer is not self-preserving. Ma and Warhaft argue that the flow is not consistent with self-similarity by demonstrating that the heat flux predicted by the similarity solution, which depends on the estimated growth rate of the layer width, differs significantly from the laboratory data.

To determine under what conditions a similarity solution for the mixing layer can exist, let $x = x/M$ be the nondimensional streamwise coordinate, $\mathcal{U}(x)$ be the characteristic scale of the velocity fluctuations, $\delta(x)$ be the length scale of the mean temperature field, and define the similarity variable $\eta = y/\delta(x)$. Since it will not affect the discussion, the characteristic scale of the mean temperature (\bar{T}) is taken to be unity. Then assume the self-similar forms

$$\bar{T} = F(\eta), \tag{2a}$$

$$\overline{u\theta} = \mathcal{U}(x)G(\eta). \tag{2b}$$

Substituting (2) into the Reynolds averaged scalar transport equation, ignoring the molecular diffusion term, shows that $(1/\mathcal{U})(d\delta/dx)$ must be constant for similarity to occur. Hence, if $\mathcal{U} \propto x^n$ and $\delta \propto x^m$, then $m - n = 1$ must hold if similarity exists. Inclusion of the molecular diffusion term in the transport equation yields the condition $\mathcal{U}\delta = \text{constant}$. This further limits the similarity solution to the case of $n = -1/2$ and $m = 1/2$. Self-similar behavior is then not expected for the cases where $\mathcal{U} \propto x^n$ and $n \neq -1/2$. In particular, this applies to the cases of nondecaying turbulence and to the decaying turbulence of the experiment of Ma and Warhaft,⁸ in which $m \approx 0.32$ and $n \approx -0.68$.

The form of the similarity equation for the mean scalar, with $(\)'$ denoting a derivative with respect to η , is

$$-\frac{\partial \delta}{\partial x} \eta F' + \mathcal{U}G' - \frac{1}{\text{Pe}_M \delta} F'' = 0, \tag{3}$$

where $\text{Pe}_M = \bar{U}M/D$ is the Peclet number, \bar{U} is the mean streamwise velocity, and D is the molecular diffusivity. In

order to compute the similarity solution for the heat flux, as was done by Ma and Warhaft, it is necessary to determine G , which can be done by assuming a form for F . Analysis of the laboratory data suggests

$$F = \frac{1}{2} [\text{erf}(\eta) + 1], \tag{4}$$

which is the same expression obtained by relating G to F through a constant eddy diffusivity and integrating (3).

Assuming that (4) is an adequate approximation for F , using $\delta = Ax^m$, $\mathcal{U} = Bx^{(m-1)}$, and (3), and noting that $G(\eta \rightarrow \infty) = 0$ yields

$$G = \frac{Am}{2B\sqrt{\pi}} \left[1 - \frac{2}{\text{Pe}_M} \frac{x^{(1-2m)}}{A^2 m} \right] \exp(-\eta^2). \tag{5}$$

Only when $m = 1/2$ is G purely a function of η , but it is informative to examine the conditions necessary for the x dependence of G to be negligibly small, namely

$$\frac{x^{(1-2m)}}{\text{Pe}_M m} \ll 1, \tag{6}$$

assuming A is order unity ($A = 0.48$ for the experiment of Ma and Warhaft). Clearly, as $\text{Pe}_M \rightarrow \infty$, the x dependence of G approaches zero for finite x . For finite Pe_M , the validity of (6) depends on the magnitude of m . In decaying, homogeneous turbulence at laboratory Reynolds numbers, the characteristic length scale of the velocity field is proportional to x^m with $m < 1/2$,^{8,12,20,21} and Ma and Warhaft⁸ show that the velocity and scalar length scales in the scalar mixing layer grow at approximately the same rate. Therefore, the exponent in (6) is positive and the x -dependence of G becomes more significant with increasing downstream distance. LaRue and Libby⁶ and LaRue *et al.*⁷ argue that the failure of the self-similar solution to match their laboratory data is due to an offset between the virtual origin of the velocity field and the virtual origin of the scalar field, and Ma and Warhaft⁸ explore this possibility experimentally by initializing the scalar field with a mandolin downstream of the grid. The implication of arguing that an offset in the virtual origin is the cause of the difference between the similarity prediction and the laboratory data for the heat flux is that, as downstream distance increases, the virtual origin error will become less significant, and similarity will be observed. Equation (6) suggests that the effects of finite Pe_M and $m \neq 1/2$ will cause the deviation between the similarity solution and the laboratory data to increase with downstream distance.

Even if it is assumed that G is not a function of x , there remains the problem of determining the appropriate value of m from the laboratory data because δ/l is not quite independent of downstream distance for the range of x/M measured. In computing the heat flux predicted by the similarity solution, Ma and Warhaft⁸ use $m = 0.32$, and note that this value results in a 25% difference between the heat flux on the centerline as predicted from similarity analysis, and that measured. They conclude from this that the flow is not consistent with self-similarity. Lumley⁹ approaches the similarity issue by assuming that the flow is not self-preserving, and

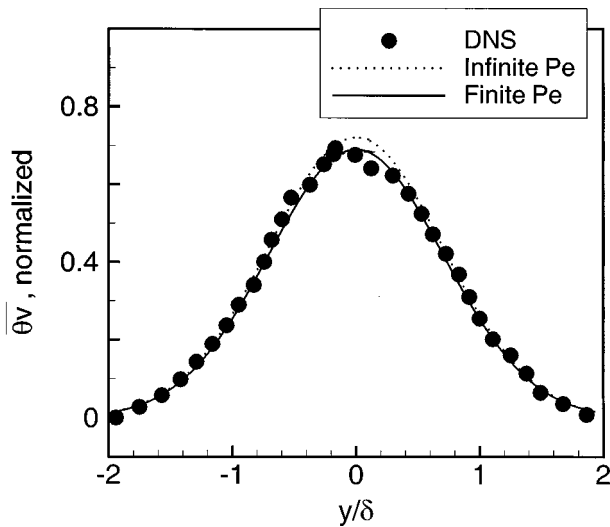


FIG. 9. Thermal flux profiles, normalized by $I_{\max} \sqrt{v^2}$, at $x/M=231$ from DNS and similarity predictions.

uses a Gram–Charlier expansion to compute the mean scalar profile as an error function plus a series of correction terms. He then integrates the heat flux profile to determine the streamwise derivative of δ , for which the corresponding decay parameter at $x/M=100$ is $m=0.25$.⁸ Inserting $m=0.25$ into (5) (with the molecular diffusion term omitted) results in a prediction of the centerline heat flux about 7% lower than in the data. Lumley includes several additional terms from the Gram–Charlier expansion to correct the prediction so that it very closely agrees with the data. The important point is that (5) is sensitive to m , and m is difficult to determine from the laboratory data.

In the direct numerical simulations, m can be determined with greater certainty than in the laboratory due to three factors. First, the virtual origins of the velocity and scalar fields are nearly aligned through the iterative procedure previously described, so that the residual mismatch in the virtual origins has a minimal impact on the growth of the layer width. Second, δ can be measured over a much larger range of x/M in the DNS than in the laboratory, which allows the flow to be observed for $\int_{t_1}^{t_2} u_{\text{rms}}/l dt = 4.4$, where t_1 and t_2 are the times at which the first and last data are measured, compared with about 1.5 for the data of Ma and Warhaft. The third factor is strictly a numerical one; in the DNS, δ can be computed at an almost unlimited number of downstream locations, compared with the relatively small number of points that can be collected practicably in the laboratory. The layer growth rate is determined by computing the three parameters needed to fit $\delta = A[(x-x_0)/M]^m$ to the data. Since the value of m is strongly influenced by the value of x_0 , it is likely that m will be more accurately determined when the curve fit involves a large amount of data, i.e., from the DNS data.

As was done for the laboratory data, the predictions for the heat flux from (5) are compared with the DNS data; the results are shown in Fig. 9 for $x/M=231$. When molecular diffusion is taken into account, (5) predicts the measured flux very closely. If the Peclet number is taken to be infinite, the similarity solution overpredicts the measured values by about

4.5% on the centerline. The molecular diffusion term in the (local) scalar transport equation can also be computed at each point in the DNS field, and averaged to yield the diffusive transport profile; in the DNS, the molecular diffusion term is 4.7% of the turbulent transport term on average at the centerline at $x/M=231$. In summary, the DNS data are almost self-preserving, but molecular diffusion effects are sufficiently large that the flow is not consistent with self-similar behavior.

V. LARGE-EDDY SIMULATIONS

The laboratory experiments of the scalar mixing layer have been limited to moderate Peclet numbers, so that testing theories based upon the infinite Peclet number against laboratory data is problematic. As noted above, limited wind tunnel length and difficulties aligning the virtual origins of the scalar and velocity fields also complicate the interpretation of experimental results. Large-eddy simulations, however, overcome all of these problems, and are well suited for examining self-similarity because the large-scale statistics of interest are insensitive to the exact form of the subgrid-scale flux models.¹¹

Chasnov¹¹ used LES to examine a passive field with and without a mean scalar gradient, and two related simulations are performed as part of our research to study the mixing layer. The same pseudo-spectral code used for the DNS is employed for these simulations, and the transport equations for momentum and scalar are augmented with a Smagorinsky term²² to represent the subgrid-scale fluxes. In the first simulation, the velocity field is initialized with an energy spectrum proportional to k^2 ; the scalar field is initialized with an error function having a δ of 2 grid points. The numerical domain is $256 \times 256 \times 512$ grid points. The simulation evolves in time with molecular viscosity and diffusivity of zero and the subgrid-scale viscosity and diffusivity determined by the Smagorinsky model. At various times, the complete three-dimensional kinetic energy spectrum is estimated by fitting (1) to the resolved part of the spectrum computed by the LES, and u_{rms} is computed from the curve-fit spectrum. From the u_{rms} obtained in this manner, the velocity decay exponent is determined to be $n = -0.664$, which is very close to the value determined by Chasnov,¹¹ and is between the value of -0.625 found by Comte-Bellot and Corrsin¹² and -0.67 found by Warhaft and Lumley.²⁰ The growth exponent of the scalar profile width is $m = 0.345$.

In the laboratory experiments and DNS, it is convenient to test for self-similarity by comparing the predicted and actual profiles of the normalized heat flux. In the LES, this is not convenient because the subgrid-scale portions of the heat flux, of the intensity of the scalar fluctuations, and of the rms of the transverse velocity fluctuations all must be modeled, and products of modeled quantities may contain errors which bias conclusions drawn from them. In the LES, however, $\int_{t_1}^{t_2} u_{\text{rms}}/l dt \approx 70$, which is such a long time that self-preservation can be determined directly by computing $m-n$ and comparing the result with the value required for similarity (unity). Fitting a power law to the LES data for

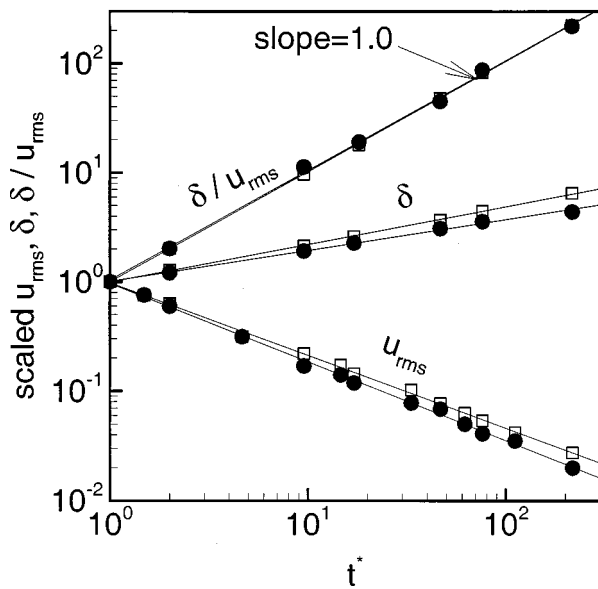


FIG. 10. Width of the mean temperature profile and rms velocity from LES of scalar mixing layer with very high Peclet number. Open and filled symbols indicate an initial kinetic energy spectra proportional to k^2 and k^4 , respectively.

δ/u_{rms} yields $m-n=1.008$. The results of the simulation are summarized in Fig. 10, where $t^*=t(u_{rms}/l)|_{t=0}$, and u_{rms} and δ are scaled by their values at $t^*=1$.

A second simulation is run with the initial kinetic energy spectrum proportional to k^4 . The velocity decay exponent in this case is $n=-0.718$, which is slightly larger in magnitude than that determined numerically by Chasnov, but is very close to the theoretical value of $-5/7$.¹¹ The mean scalar profile width grows with $m=0.285$, and the least-squares fit to the ratio δ/u_{rms} yields $m-n=1.004$. The results are summarized in Fig. 10. The large-eddy simulations indicate that the evolution of a scalar mixing layer in homogeneous, isotropic turbulence is consistent with the similarity solution determined by omitting the diffusion term in the scalar transport equation, i.e., $m-n=1$, regardless of the rate at which the velocity field decays. Both the decay rate of u_{rms} and the spreading rate of the mean scalar profile remain constant as the length scales in the problem increase and the smallest length scale resolved in the LES becomes a smaller and smaller fraction of the integral length scale.

VI. CONCLUSIONS

The question of whether a temperature mixing layer evolves in a self-similar manner is of importance in developing and validating theories about scalar mixing. The simplicity of the flow encourages the thought that it is self-similar, but several laboratory experiments at moderate Peclet numbers have found that the flow is not self-preserving. This conclusion is based on the fact that the heat flux computed using the similarity-solution and the observed growth rate of the mixing layer is not consistent with the measured heat flux.⁸

The DNS results are consistent with the laboratory findings that a mixing layer at a moderate Peclet number does

not evolve in a self-similar manner. In the DNS, the growth rate of the mixing layer can be determined with greater confidence than in the laboratory experiment, and the difference between the heat flux consistent with similarity and that measured is only about 4.5%. For the Reynolds averaged transport equations, however, a similarity solution at a moderate Peclet number can only be attained for a specific kinetic energy decay rate, which is not observed in the laboratory. In the DNS, the molecular diffusive transport of the heat is computed directly, and found to be 4.7% of the turbulent transport, or approximately equal to the mismatch between the similarity solution and the measured heat flux. Two large-eddy simulations with the molecular diffusivity set to zero and different kinetic energy decay rates indicate that the mixing layer at a very high Peclet number does evolve in a self-similar manner, as expected from similarity analysis of the Reynolds averaged transport equations with the diffusion term omitted.

The results from this research, combined with those of the previously cited laboratory experiments by other researchers, suggest three conclusions concerning self-preservation of the thermal mixing layer: (1) the mixing layer at a moderate Peclet number is not self-similar due to the effects of molecular diffusion, (2) the mixing layer at a high Peclet number is self-similar, and (3) the small deviation from self-similarity expected in the laboratory data due to molecular diffusion is obscured because it is difficult to accurately determine the growth rate of the layer.⁸ In addition, the DNS data support the argument presented in another paper that isotropic turbulence can be accurately simulated,¹⁰ and the LES results demonstrate the value of that simulation technique in basic research.

ACKNOWLEDGMENTS

This work was supported by the National Science Foundation (Grant No. CTS9810103) and the Air Force Office of Scientific Research (Grant No. F49620-97-1-0092). High performance computer (HPC) resources were generously provided by the Arctic Region Supercomputing Center.

¹R. W. Bilger, L. R. Sætran, and L. V. Krishnamoorthy, "Reaction in a scalar mixing layer," *J. Fluid Mech.* **233**, 211 (1991).

²J. D. Li, R. J. Brown, and R. W. Bilger, "Experimental study of a scalar mixing layer using reactive and passive scalars," in *11th Australasian Fluid Mechanics Conference*, Hobart, 1992, pp. 159–162.

³W. E. Watt and W. D. Baines, "The turbulent temperature mixing layer," *J. Hydraul. Res.* **11**, 158 (1973).

⁴J. Foss, J. Schlein, and S. Corrsin, unpublished, 1975.

⁵P. A. Libby, "Diffusion of heat downstream of a turbulence grid," *Acta Astron.* **2**, 867 (1975).

⁶J. C. LaRue and P. A. Libby, "Thermal mixing layer downstream of half-heated turbulence grid," *Phys. Fluids* **24**, 597 (1981).

⁷J. C. LaRue, P. A. Libby, and D. V. R. Seshadri, "Further results on the thermal mixing layer downstream of a turbulence grid," *Phys. Fluids* **24**, 1927 (1981).

⁸B.-K. Ma and Z. Warhaft, "Some aspects of the thermal mixing layer in grid turbulence," *Phys. Fluids* **29**, 3114 (1986).

⁹J. L. Lumley, "Evolution of non-self-preserving thermal mixing layer," *Phys. Fluids* **29**, 3976 (1986).

¹⁰S. M. de Bruyn Kops, and J. J. Riley, "Direct numerical simulation of laboratory experiments in isotropic turbulence," *Phys. Fluids* **10**, 2125 (1998).

- ¹¹J. R. Chasnov, "Similarity states of passive scalar transport in isotropic turbulence," *Phys. Fluids* **6**, 1036 (1994).
- ¹²G. Comte-Bellot and S. Corrsin, "Simple Eulerian time correlation of full and narrow-band velocity signals in grid-generated, 'isotropic' turbulence," *J. Fluid Mech.* **48**, 273 (1971).
- ¹³A. Sirivat and Z. Warhaft, "The effect of a passive cross-stream temperature gradient on the evolution of temperature variance and heat flux in grid turbulence," *J. Fluid Mech.* **128**, 323 (1983).
- ¹⁴H. Tennekes and J. L. Lumley, *A First Course in Turbulence* (MIT Press, Cambridge, 1972).
- ¹⁵S. Corrsin, "Further generalizations of Onsager's cascade model for turbulent spectra," *Phys. Fluids* **7**, 1156 (1964).
- ¹⁶G. K. Batchelor, *The Theory of Homogeneous Turbulence* (Cambridge University Press, London, 1953).
- ¹⁷S. Tavoularis, J. C. Bennett, and S. Corrsin, "Velocity-derivative skewness in small Reynolds number, nearly isotropic turbulence," *J. Fluid Mech.* **88**, 63 (1978).
- ¹⁸S. E. Elghobashi and B. E. Launder, "Turbulent time scales and the dissipation rate of temperature variance in the thermal mixing layer," *Phys. Fluids* **26**, 2415 (1983).
- ¹⁹J. M. MacInnes, "Numerical simulation of the thermal turbulent mixing layer," *Phys. Fluids* **28**, 1013 (1985).
- ²⁰Z. Warhaft and J. L. Lumley, "An experimental study of the decay of temperature fluctuations in grid-generated turbulence," *J. Fluid Mech.* **88**, 659 (1978).
- ²¹K. R. Sreenivasan, S. Tavoularis, R. Henry, and S. Corrsin, "Temperature fluctuations and scales in grid generated turbulence," *J. Fluid Mech.* **100**, 597 (1980).
- ²²J. Smagorinsky, "General circulation experiments with the primitive equations. I. The basic experiment.," *Mon. Weather Rev.* **91**, 99 (1963).